Distribution System State Estimation via Behavioral Modeling of Distributed Energy Resources

Muneeb Mushtaq Sheikh, *Graduate Student Member, IEEE*, Himani Mattoo, *Member, IEEE*, Sreenath J G, *Member, IEEE*

***Abstract*—The proliferation of distributed energy resources (DERs) and demand response (DR) programs introduces significant uncertainties in the monitoring of the distribution system. This paper proposes a novel forecasting-aided state estimation (FASE) framework that integrates behavioral modeling of aggregated DERs with dynamic state tracking. The approach employs subspace identification to derive compact state-space representations, embedded within a hybrid Unscented Kalman Filter (UKF) architecture for refined measurement generation. Validation on the IEEE-123 bus system demonstrates 65.8% improvement in voltage estimation accuracy compared to conventional methods and maintains robust performance under 40% measurement loss scenarios. The framework provides enhanced observability during rapid load-generation fluctuations and communication disruptions, offering a critical foundation for real-time distribution network management.**

***Index Terms*—Power system state estimation, distributed energy resources, demand response.**

I. Introduction

As distributed energy resources (DERs) and responsive loads continue to expand across distribution networks, the variability in consumption patterns has increased significantly. This variability is further compounded by the growing presence of distributed resources located at the end-load (DRELs), such as customer-owned generation and storage units, which introduce additional uncertainty into feeder behaviour [1]. These evolving characteristics reduce the predictability of network conditions and complicate real-time monitoring. Therefore, it necessitates the need for approaches that can maintain observability and support reliable system monitoring.

Traditional static state estimation (SE) techniques are not well-suited to capture the rapidly evolving behaviour of active distribution networks (ADNs). It motivates the shift toward dynamic SE methods [2]. Among these, forecasting-aided state estimation (FASE) offers a compelling approach by utilizing information from previous system states to predict future system states [3]. This predictive capability becomes especially important in networks with substantial penetration of DERs and DRELs, where rapid fluctuations and uncertain load–generation interactions must be accurately anticipated.

To realize the potential of FASE and other dynamic SE methods in ADNs, accurate pseudo-measurement modelling remains a key challenge. Accurate pseudo-measurement modelling remains a key challenge. Existing pseudo-measurement approaches rely heavily on historical profiles, which can deviate substantially from actual operating conditions [4]. Statistical and probabilistic approaches, such as Gaussian assumptions [5] or Gaussian mixture models (GMMs) [6] have been employed. Although effective to an extent, these methods may degrade SE accuracy under high variability or multimodal load distributions [7]. Maximum likelihood–based approaches improve modelling flexibility but may encounter numerical instability under unfavourable measurement conditions [8]. In parallel, machine-learning-based solutions, such as probabilistic neural networks (PNNs) [9] and autoregressive fusion models [10], use real-time data to improve pseudo-measurements. However, they still face difficulty capturing the stochastic behaviour of DRELs and customer-controlled devices, which strongly influence net demand [11]. Sudden load changes, ramp events, and diverse consumer actions further introduce unpredictable deviations, highlighting the need for more robust and adaptive modelling strategies.

Furthermore, all the existing pseudo-measurement-based approaches for static SE typically rely on fixed consumption profiles associated with different customer classes [12]. However, these methods do not sufficiently capture the variability introduced by demand response (DR) programs and DRELs, both of which can produce operating behaviours that deviate markedly from traditional consumption patterns [1]. This growing variability calls for modelling approaches that track the changing dynamics of ADNs.

This work incorporates an explicit representation of end-load resource (DREL) behaviour into the distribution system SE (DSSE) pipeline. The proposed approach combines two complementary elements. First, a deep-learning forecasting module produces short-term, aggregated nodal demand forecasts that capture DREL-driven fluctuations using limited measurements together with weather and price signals [3]. Second, a compact node-level behavioural model consolidates local DER dynamics, DR participation and end-load characteristics into an input–output representation suitable for real-time SE.

Node-level behavioural models are identified from historical measurements, price-response records and meteorological data using a numerical subspace state-space identification procedure. Each model is validated on hold-out data prior to deployment. Validated models are embedded in an Unscented Kalman Filter (UKF) [13] to refine noisy remote terminal unit (RTU) measurements and supply high-quality new measurements. The UKF prediction–correction cycle is then integrated within a FASE framework to obtain network states. By treating DREL activity as a predictable component rather than an unstruc-

This work was partially supported by Grid Controller of India Limited, NERLDC [Project No. xEEEICNGRID00840xxPT001]

The authors are with the Department of Electronics and Electrical Engineering, IIT Guwahati, Guwahati 781039, India (e-mail: s.muneeb@iitg.ac.in, hmattoo@iitg.ac.in, sreenathjg@iitg.ac.in)

979-8-3315-8138-1

tured disturbance, the framework improves observability and increases resilience to temporary communication outages.

The main contributions of this work are:

- A node-level behavioural modelling framework that compactly captures feeder dynamics induced by DRELs and other distributed resources.
- A hybrid forecasting and filtering scheme that refines real-time measurements and supplies model-based refined measurements via UKF integration.
- Enhanced DSSE robustness under measurement sparsity and communication delays through the coordinated FASE architecture.

II. Modeling of Distributed Energy Resources

A. Subspace Identification Framework

Modern distribution systems require modeling the collective influence of numerous DERs without explicitly representing each device [10], [11]. To achieve this, a behavioral state-space model is developed using subspace identification, which derives system dynamics directly from historical input–output data without assuming a predefined structure.

The state vector $\mathbf{x}_k^b \in \mathbb{R}^q$ represents the aggregate operational behavior of resources such as photovoltaic units (PVs), electric vehicles (EVs), and flexible loads. The superscript b denotes behavioral states, and the model evolves as

$$\mathbf{x}_k^b = \mathbf{A}\mathbf{x}_{k-1}^b + \mathbf{B}\mathbf{u}_{k-1}^{\mathrm{ext}} + \mathbf{w}_{k-1}^b, \tag{1}$$

where $\mathbf{A}$ and $\mathbf{B}$ denote the state transition and input matrices, respectively, and $\mathbf{w}_k^b \sim \mathcal{N}(0, \mathbf{Q}^b)$ captures unmodeled variations. The main factors influencing PV operation in our case study, solar irradiance I_k, ambient temperature T_k, and electricity price deviation $\Delta\pi_k$, are included in the external input vector $\mathbf{u}_k^{\mathrm{ext}} = [\Delta\pi_k, T_k, I_k]^\top$. The measurable output can be expressed as follows:

$$\mathbf{y}_k = \mathbf{C}\mathbf{x}_k^b + \mathbf{D}\mathbf{u}_k^{\mathrm{ext}} + \mathbf{v}_k, \tag{2}$$

where $\mathbf{v}_k \sim \mathcal{N}(0, \mathbf{R}^b)$ represents measurement noise, $\mathbf{D}$ captures direct input effects, and $\mathbf{C}$ maps latent states to observable power injections.

By capturing temporal correlations and the impact of external variables like price and weather, this formulation offers a data-driven depiction of aggregate DER behavior. In order to ensure robustness and consistency, a structured four-step subspace identification approach is used to identify the matrices $\mathbf{A}$, $\mathbf{B}$, $\mathbf{C}$, and $\mathbf{D}$.

B. Four-Step Identification Procedure

1) Step 1: Data Structuring: To capture temporal dependencies, historical input $\mathbf{u}_k$ and output $\mathbf{y}_k$ are grouped into block Hankel matrices $\mathbf{U}_p$ and $\mathbf{Y}_f$.

$$\mathbf{U}_p = \begin{bmatrix} \mathbf{u}_0 & \cdots & \mathbf{u}_{j-1} \\ \vdots & \ddots & \vdots \\ \mathbf{u}_{i-1} & \cdots & \mathbf{u}_{i+j-2} \end{bmatrix}, \mathbf{Y}_f = \begin{bmatrix} \mathbf{y}_i & \cdots & \mathbf{y}_{i+j-1} \\ \vdots & \ddots & \vdots \\ \mathbf{y}_{2i-1} & \cdots & \mathbf{y}_{2i+j-2} \end{bmatrix} \tag{3}$$

The temporal resolution and an upper bound on the model order are defined by the window length i.

2) Step 2: Oblique Projection: This process isolates the internal dynamics of the system by separating the part of future outputs that can be anticipated from historical data. The expression for the oblique projection is

$$\mathcal{P} = \mathbf{Y}_f /_{\mathbf{U}_f} \mathbf{W}_p, \tag{4}$$

where $\mathrm{W}_p = [\mathbf{U}_p^\top, \mathbf{Y}_p^\top]^\top$ merges previous inputs and outputs. In order to improve numerical stability and prevent direct inversion, the projection is calculated via a LQ decomposition.

3) Step 3: State Sequence Extraction via Singular Value Decomposition: The projection matrix $\mathcal{P}$ encapsulates the system's dominant dynamic behavior. Singular value decomposition is applied as

$$\mathcal{P} = \mathbf{U}\mathbf{\Sigma}\mathbf{V}^\top = [\mathbf{U}_1 \ \mathbf{U}_2] \begin{bmatrix} \mathbf{\Sigma}_1 & \mathbf{0} \\ \mathbf{0} & \mathbf{\Sigma}_2 \end{bmatrix} \begin{bmatrix} \mathbf{V}_1^\top \\ \mathbf{V}_2^\top \end{bmatrix}, \tag{5}$$

where $\mathbf{\Sigma}$ is a diagonal matrix of singular values ordered in decreasing order, and $\mathbf{U}$ and $\mathbf{V}$ are orthogonal matrices holding the left and right singular vectors of $\mathcal{P}$. The q_m biggest singular values gathered in $\mathbf{\Sigma}_1$ are represented by the matrices $\mathbf{U}_1, \mathbf{V}_1$, whereas the smaller, truncated modes are represented by $\mathbf{U}_2, \mathbf{V}_2$. Next, the state sequence is estimated as

$$\mathbf{X}_f^b = \mathbf{\Sigma}_1^{1/2}\mathbf{V}_1^\top, \tag{6}$$

where each column of $\mathbf{X}_f^b \in \mathbb{R}^{q_m \times j}$ represents the behavioral state at a particular time. A compact yet accurate state representation is ensured by choosing the maintained order q_m so that the cumulative energy of $\mathbf{\Sigma}_1$ captures at least 95–99% of the overall singular value energy.

4) Step 4: System Matrix Estimation via Least Squares: After determining $\mathbf{X}_f^b$, a least-squares regression between the shifted state, input, and output data is solved to estimate the system matrices:

$$\begin{bmatrix} \mathbf{X}_{k+1}^b \\ \mathbf{Y}_k \end{bmatrix} = \begin{bmatrix} \mathbf{A} & \mathbf{B} \\ \mathbf{C} & \mathbf{D} \end{bmatrix} \begin{bmatrix} \mathbf{X}_k^b \\ \mathbf{U}_k \end{bmatrix} + \begin{bmatrix} \boldsymbol{\rho}_w \\ \boldsymbol{\rho}_v \end{bmatrix}, \tag{7}$$

where residuals are represented by $\boldsymbol{\rho}_w$ and $\boldsymbol{\rho}_v$. The least-squares estimate that minimizes $\|\boldsymbol{\rho}_w\|_F^2 + \|\boldsymbol{\rho}_v|_F^2$ is provided by

$$\begin{bmatrix} \mathbf{A} & \mathbf{B} \\ \mathbf{C} & \mathbf{D} \end{bmatrix} = \begin{bmatrix} \mathbf{X}_{k+1}^b \\ \mathbf{Y}_k \end{bmatrix} \begin{bmatrix} \mathbf{X}_k^b \\ \mathbf{U}_k \end{bmatrix}^\top \left(\begin{bmatrix} \mathbf{X}_k^b \\ \mathbf{U}_k \end{bmatrix} \begin{bmatrix} \mathbf{X}_k^b \\ \mathbf{U}_k \end{bmatrix}^\top \right)^{-1}. \tag{8}$$

This expression completes the data-driven building of the predictive state-space model by directly connecting the estimated system matrices to measured data.

III. Two-Stage Predictive Estimation Framework

The behavioral SE uses a UKF to capture nonlinear demand patterns in the framework's dual-filter design, producing refined measurements based on behavioral modeling. The electrical SE employs an EKF to efficiently track system states after receiving these revised measurements [13], [14]. This hybrid design takes advantage of the EKF's computing efficiency for the near-linear electrical state dynamics while utilizing the UKF's capacity to propagate the mean and covariance of nonlinear demand behavior.

979-8-3315-8138-1

A. Behavioral SE via UKF

Using the subspace-identified state-space model, the behavioral SE uses a UKF to monitor latent DER dynamics:

$$\mathbf{x}_k^b = \mathbf{A}\mathbf{x}_{k-1}^b + \mathbf{B}\mathbf{u}_{k-1}^{\text{ext}} + \mathbf{K}\mathbf{r}_{k-1} + \mathbf{w}_{k-1}^b, \tag{9}$$
$$\mathbf{z}_k^b = \mathbf{C}\mathbf{x}_k^b + \mathbf{D}\bar{\mathbf{u}}_k + \mathbf{v}_k^b. \tag{10}$$

where $\mathbf{A}, \mathbf{B}, \mathbf{C}, \mathbf{D}$ are system matrices found using the subspace procedure, $\mathbf{K}$ is the Kalman gain matrix, $\mathbf{r}_{k-1}$ stands for residuals, $\mathbf{w}_{k-1}^b \sim \mathcal{N}(0, \mathbf{Q}^b)$ is process noise, and $\mathbf{v}_k^b \sim \mathcal{N}(0, \mathbf{R}^b)$ is measurement noise. The input $\bar{\mathbf{u}}_k$ denotes forecasted external inputs obtained through auxiliary forecasting techniques. The UKF implementation follows a systematic procedure beginning with sigma point generation around the previous state estimate:

$$\chi_{k-1}^{(i)} = \hat{\mathbf{x}}_{k-1}^b \pm \sqrt{(n_b + \lambda)\hat{\mathbf{P}}_{k-1}^b}_i \quad \text{for } i = 1, \ldots, 2n_b \tag{11}$$

where n_b is the behavioral state dimension, λ is a scaling parameter, and $\hat{\mathbf{P}}_{k-1}^b$ is the state covariance matrix. These sigma points are then propagated as:

$$\chi_{k|k-1}^{(i)} = \mathbf{A}\chi_{k-1}^{(i)} + \mathbf{B}\mathbf{u}_{k-1}^{\text{ext}} + \mathbf{K}\mathbf{r}_{k-1} \tag{12}$$

The predicted state mean and covariance are computed through weighted averaging:

$$\tilde{\mathbf{x}}_k^b = \sum_{i=0}^{2n_b} W_i^{(m)} \chi_{k|k-1}^{(i)} \tag{13}$$
$$\tilde{\mathbf{P}}_k^b = \sum_{i=0}^{2n_b} W_i^{(c)} (\chi_{k|k-1}^{(i)} - \tilde{\mathbf{x}}_k^b)(\chi_{k|k-1}^{(i)} - \tilde{\mathbf{x}}_k^b)^\top + \mathbf{Q}^b \tag{14}$$

where $W_i^{(m)}$ and $W_i^{(c)}$ are carefully chosen weights that preserve the statistical properties of the transformed distribution.

Measurement prediction follows a similar pattern, with sigma points transformed through the output equation:

$$\mathcal{Z}_{k|k-1}^{(i)} = \mathbf{C}\chi_{k|k-1}^{(i)} + \mathbf{D}\bar{\mathbf{u}}_k \tag{15}$$

The predicted measurement mean and covariance are:

$$\tilde{\mathbf{z}}_k^b = \sum_{i=0}^{2n_b} W_i^{(m)} \mathcal{Z}_{k|k-1}^{(i)} \tag{16}$$
$$\tilde{\mathbf{P}}_k^{z,b} = \sum_{i=0}^{2n_b} W_i^{(c)} (\mathcal{Z}_{k|k-1}^{(i)} - \tilde{\mathbf{z}}_k^b)(\mathcal{Z}_{k|k-1}^{(i)} - \tilde{\mathbf{z}}_k^b)^\top + \mathbf{R}^b \tag{17}$$

The cross-covariance (Eqn. 18) between state and measurement predictions enables Kalman gain computation (Eqn. 19) as given respectively as:

$$\tilde{\mathbf{P}}_k^{b,z} = \sum_{i=0}^{2n_b} W_i^{(c)} (\chi_{k|k-1}^{(i)} - \tilde{\mathbf{x}}_k^b)(\mathcal{Z}_{k|k-1}^{(i)} - \tilde{\mathbf{z}}_k^b)^\top, \quad \mathbf{K}_k^b = \tilde{\mathbf{P}}_k^{b,z}(\tilde{\mathbf{P}}_k^{z,b})^{-1} \tag{18,19}$$

Finally, the behavioral state estimate is updated through measurement incorporation as:

$$\hat{\mathbf{x}}_k^b = \tilde{\mathbf{x}}_k^b + \mathbf{K}_k^b(\mathbf{z}_k^b - \tilde{\mathbf{z}}_k^b), \quad \hat{\mathbf{P}}_k^b = \tilde{\mathbf{P}}_k^b - \mathbf{K}_k^b \tilde{\mathbf{P}}_k^{z,b}(\mathbf{K}_k^b).^\top \tag{20}$$

This UKF-based behavioral tracking provides refined demand estimates and uncertainty quantification essential for subsequent electrical SE.

B. Electrical SE via Forecasting-Aided EKF

The electrical SE adopts a forecasting-aided EKF framework to track nodal voltage magnitudes and angles across the distribution network [14]. The state transition model integrates both physical dynamics and behavioral influences, given by

$$\mathbf{x}_k^{\text{elec}} = \mathbf{F}_{k-1}\mathbf{x}_{k-1}^{\text{elec}} + \mathbf{g}_{k-1} + \mathbf{w}_{k-1}^{\text{elec}}, \tag{21}$$
$$\mathbf{z}_k^{\text{elec}} = h(\mathbf{x}_k^{\text{elec}}) + \mathbf{v}_k^{\text{elec}}, \tag{22}$$

where $\mathbf{F}_{k-1}$ and $\mathbf{g}_{k-1}$ denote the state transition matrix and the system trajectory vector incorporating DR effects, respectively, both obtained using the Holt method [14]; $h(\cdot)$ represents the nonlinear power flow model; $\mathbf{w}_{k-1}^{\text{elec}} \sim \mathcal{N}(0, \mathbf{Q}^{\text{elec}})$ denotes the process noise; and $\mathbf{v}_k^{\text{elec}} \sim \mathcal{N}(0, \mathbf{R}^{\text{elec}})$ represents the measurement noise.

The EKF prediction step propagates the electrical state estimate and covariance, respectively, as:

$$\tilde{\mathbf{x}}_k^{\text{elec}} = \mathbf{F}_{k-1}\hat{\mathbf{x}}_{k-1}^{\text{elec}} + \mathbf{g}_{k-1}, \quad \tilde{\mathbf{P}}_k^{\text{elec}} = \mathbf{F}_{k-1}\hat{\mathbf{P}}_{k-1}^{\text{elec}}\mathbf{F}_{k-1}^\top + \mathbf{Q}^{\text{elec}}, \tag{23,24}$$

To account for uncertainty in behavioral forecasts, an adaptive measurement covariance is introduced:

$$\mathbf{R}_k^{\text{DR}} = \text{diag}\big(\sigma_{\text{DR},j,k}^2\big), \quad \sigma_{\text{DR},j,k}^2 = \gamma_{\text{DR}} P_{0,j}^2 + \mathbf{C}^{(j)}\tilde{\mathbf{P}}_k^b(\mathbf{C}^{(j)})^\top, \tag{25,26}$$

where $\mathcal{B}^{\text{DR}}$ denotes the set of DR-enabled buses, $P_{0,j}$ is the nominal demand at bus j, and γ_{DR} sets the baseline DR uncertainty (typically 10^{-4}–10^{-2}). Here, $\tilde{\mathbf{P}}_k^b$ denotes the predicted behavioral-state covariance, while $\mathbf{C}^{(j)}$ extracts its contribution at bus j. Consequently, $\sigma_{\text{DR},j,k}^2$ accounts for both inherent demand variability and behavioral forecast uncertainty. This adaptive formulation dynamically regulates measurement confidence, ensuring balanced weighting between real measurements and behavioral predictions. The EKF update equations complete the electrical SE and are given as:

$$\mathbf{K}_k^{\text{elec}} = \tilde{\mathbf{P}}_k^{\text{elec}}\mathbf{H}_k^\top(\mathbf{H}_k\tilde{\mathbf{P}}_k^{\text{elec}}\mathbf{H}_k^\top + \mathbf{R}_k^{\text{DR}})^{-1}, \tag{27}$$
$$\hat{\mathbf{x}}_k^{\text{elec}} = \tilde{\mathbf{x}}_k^{\text{elec}} + \mathbf{K}_k^{\text{elec}}[\mathbf{z}_k^{\text{elec}} - h(\tilde{\mathbf{x}}_k^{\text{elec}})], \tag{28}$$
$$\hat{\mathbf{P}}_k^{\text{elec}} = (\mathbf{I} - \mathbf{K}_k^{\text{elec}}\mathbf{H}_k)\tilde{\mathbf{P}}_k^{\text{elec}}, \tag{29}$$

where $\mathbf{H}_k$ is the Jacobian of $h(\cdot)$ evaluated at $\tilde{\mathbf{x}}_k^{\text{elec}}$.

C. Boundary Coordination

Large-scale distribution networks cannot be estimated as a single region; thus SE is executed in a decentralized manner. The system is partitioned into multiple clusters, each performing local SE while maintaining global consistency through boundary information exchange [14]. Neighbouring clusters exchange boundary states, covariance matrices, and DR-related forecasts to ensure coordinated multi-area estimation. The control center of cluster m (edge estimation point (EEP)) communicates with the EEP of cluster n either periodically or upon detecting a DR-induced disturbance [19]. The transmitted packet includes the forecasted DR response at boundary buses $\mathbf{u}_{k,m}^{\text{DR},b}$, its uncertainty $\mathbf{\Sigma}_{k,m}^{\text{DR},b}$ (with entries $\sigma_{\text{DR},j,k}^2$), and the predicted activation time $\tau_{k,m}^{\text{DR}}$, along with the boundary-state estimate and its covariance. After receiving this information, the EEP of cluster n aligns $\tau_{k,m}^{\text{DR}}$ with its local prediction horizon and fuses the remaining data to maintain synchronized and consistent multi-area state estimates [14].

979-8-3315-8138-1

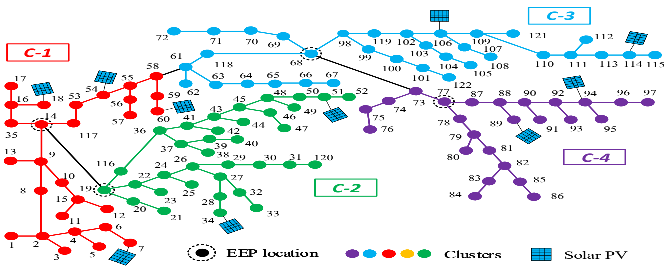

Fig. 1. Clustered IEEE 123-bus system.

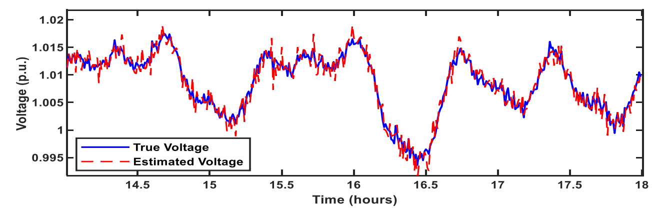

Fig. 2. Voltage magnitude tracking at Bus 18 under DR activity.

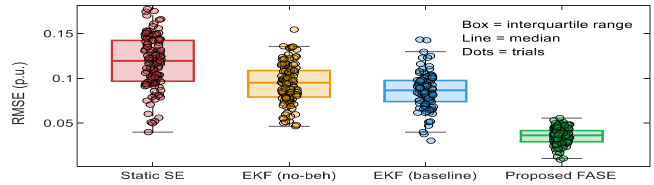

Fig. 3. Voltage RMSE across all IEEE 123-buses for four SE approaches.

TABLE I
COMPARISON OF PSEUDO-MEASUREMENT ACCURACY

Method Category	**RMSE (Active Power)**
Statistical Model [6]	0.2410 pu
Deep Learning Forecaster [3]	0.0680 pu
Proposed Framework	**0.0175 pu**

IV. NETWORK AUGMENTATION AND DATA GENERATION

The IEEE 123-bus feeder is modified to model an ADN with integrated PV and DR resources. Load and generation profiles from an 11 kV substation at IIT Kanpur are filtered to the 14:00–18:00 window and downsampled to $N = 6000$ samples. It yields a 2.4 s sampling interval that preserves PV ramps and DR transients. Simulations are performed on a desktop with an Intel Core i7-10700 CPU and 16 GB RAM.

1) DER Deployment: Ten utility-scale PV units are deployed at representative buses in the IEEE 123-bus feeder (Fig. 1), contributing approximately 15% of the system peak load. DR resources are assigned to buses 18, 34, 60, 94, and 106, accounting for 20% of controllable demand. Responsive loads follow a nonlinear price-elastic model [15], with DR events triggered during the evening PV ramp-down period (16:00–17:00). Non-DR loads follow a normalized daily profile with a 1.8:1 peak-to-trough ratio. Net active power injections include PV generation, DR curtailment, and 2–3% zero-mean Gaussian noise.

2) Measurement Configuration: Measurements are generated by perturbing true system states with additive white Gaussian noise (AWGN). RTU voltage magnitudes and power flow measurements are assigned standard deviations of 1% and 2%, respectively [16], while μPMU voltage and current phasors are corrupted with 0.01% AWGN variance in both real and imaginary components [17]. RTUs operate at 1 Hz and μPMUs at 10 Hz, whereas SE is executed at 2 Hz. Consequently, RTU data are available at alternate time instants, and pseudo-measurements are utilized otherwise. Therefore, the state estimator relies more heavily on pseudo measurements. Sensor placement and measurement types follow Ref. [18]. A three-phase unbalanced load flow is performed over 6,000 time steps ($N = 6000$) with bus 1 as the slack reference, ensuring physically consistent operating points.

V. RESULTS AND PERFORMANCE ANALYSIS

The effectiveness of the proposed FASE framework was evaluated on a test system under normal operating conditions, realistic DR activity, and under communication losses.

A. State Estimation Accuracy Under Normal Operation

The hybrid two-stage SE framework is evaluated under normal operating conditions over a 4-hour window (14:00–18:00), corresponding to the evening PV ramp-down period. Fig. 2 shows the voltage tracking at DR Bus 18, where the proposed FASE method closely follows the true trajectory throughout the operating window. Across all buses, the voltage magnitude RMSE [19] averages 0.034 pu, satisfying distribution-level accuracy requirements, while the EKF-based electrical stage remains numerically stable without divergence.

A comparative analysis against three other approaches, i.e., traditional static SE [19], an EKF without behavioural modelling [14], and an EKF using baseline demand projections, demonstrates the benefits of the proposed strategy (Fig. 3). Median RMSE in system states computed over 100 Monte Carlo runs were 0.13 pu for static SE, 0.099 pu for the decoupled EKF, 0.098 pu for the baseline-forecast EKF, and 0.0335 pu for the proposed FASE. These results correspond to performance gains of 74.2% relative to static SE, 66.2% relative to the decoupled EKF, and 65.8% relative to the baseline-forecast EKF. The substantial decrease in SE error and variance confirms that integrating behavioral modeling with electrical SE significantly improves tracking accuracy and robustness under dynamic network conditions. Furthermore, the computational efficiency of the proposed framework is assessed for real-time feasibility, yielding an average execution time of approximately 28 ms per time step per cluster.

B. Performance During DR Events

Four coordinated DR activations occured at 15:20, 16:10, 17:00, and 17:40. These events introduced high variability in nodal injections, creating conditions that typically degrade observability. The proposed behavioral model provided accurate short-term forecasts. Table I summarizes its comparative performance, demonstrating improved pseudo-measurement accuracy relative to benchmark methods. This enabled the UKF to generate high-confidence measurements and stabilize the subsequent electrical SE. Fig. 4 illustrates DR-induced active power changes at the five DR-enabled buses during a

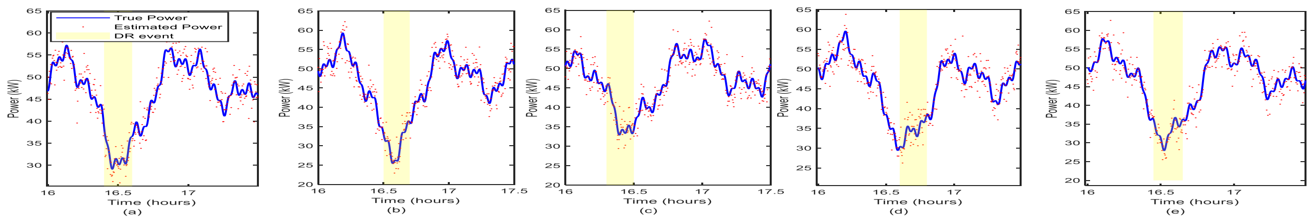

Fig. 4. DR nodal power responses for buses (a) 18, (b) 34, (c) 60, (d) 94, and (e) 106 during a curtailment event.

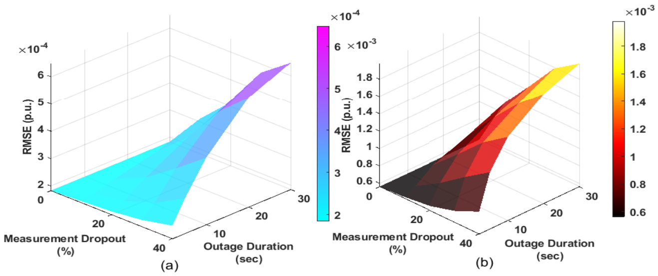

Fig. 5. Voltage estimation RMSE under 0–40% RTU outages (2–30 s). Comparison of (a) proposed FASE and (b) EKF without behavioural modelling.

representative curtailment window (16:00–17:30). Peak curtailment depths reached 28%, 32%, 25%, 31%, and 27%, consistent with the underlying price-elastic demand model. The behavioral forecaster accurately predicted 87.3% of the curtailment magnitude within a 5-minute lead, enabling proactive adjustment of Kalman gains and preserving estimation accuracy during abrupt load shifts.

C. Robustness to measurement loss and communication delays

A key advantage of the proposed FASE is its ability to retain observability under temporary measurement loss because the behavoural model through UKF predicts the refined measurements across the network that help to maintain observability and accuracy in state estimates. Monte Carlo simulations (100 runs) emulated communication outages by dropping measurement streams from 0%, 10%, 20%, 30%, and 40% of RTU-equipped buses. The percentage represents the fraction of RTU data intentionally made unavailable during the outage, with durations ranging from 2 to 30 seconds.

Fig. 5 presents voltage RMSE deterioration as a function of outage duration and measurement availability. At 20% dropout and a 10-second interruption, the RMSE of the proposed FASE increased from 0.034 pu to 0.047 pu (38.2% degradation), while EKF without behavoural modelling experienced error growth to 0.31 pu under identical conditions. Even under severe stress (40% dropout, 30 seconds), the proposed FASE maintained RMSE below 0.1 pu, compared to 0.157 pu for the benchmark method. This 57.2% improvement highlights the value of behavioral prediction during periods of measurement scarcity.

VI. Conclusion

This work develops a two-stage FASE approach designed to overcome operational challenges arising from the extensive integration of DERs and DR initiatives in ADNs. The methodology combines behavioral representations obtained through subspace system identification with UKF. Then, with EKF utilising the refined measurements from UKF, it provides the state estimates of the system. Evaluation results confirm the framework's capability to maintain reliable performance during DR events and temporary communication failures, demonstrating its practical utility in real-world distribution system operation.

References

[1] A. Srivastava et al., "Distribution System Behind-the-Meter DERs: Estimation, Uncertainty Quantification, and Control," *IEEE Trans. Power Syst.*, vol. 40, no. 1, pp. 1060-1077, Jan. 2025.

[2] Z. Fang, Y. Lin, S. Song, C. Li, X. Lin, and Y. Chen, "State estimation for situational awareness of active distribution system with photovoltaic power plants," *IEEE Trans. Smart Grid*, vol. 12, Jan. 2021.

[3] M. Alduhaymi, R. Singh, F. Ul Nazir, B. C. Pal, and A. Ahmadi, "Forecasting-aided state estimation with deep learning-generated pseudo measurements," *IEEE Trans. Instrum. Meas.*, vol. 74, pp. 1–12, 2025.

[4] A. Primadianto and C.-N. Lu, "A review on distribution system state estimation," *IEEE Trans. Power Syst.*, vol. 32, pp. 3875–3883, 2017.

[5] R. Herman et al., "The statistical description of grouped domestic electrical load currents," *Electric Power Syst. Res.*, vol. 27, 1993.

[6] R. Singh, B. C. Pal, and R. A. Jabr, "Statistical representation of distribution system loads using gaussian mixture model," *IEEE Trans. Power Syst.*, vol. 25, no. 1, pp. 29–37, Feb. 2010.

[7] A. P. Yadav et al., "Review of emerging concepts in distribution system state estimation: Opportunities and challenges," *IEEE Access,* vol. 11, pp. 70 503–70 515, 2023.

[8] M. Vanin, T. Van Acker, R. D'hulst, and D. Van Hertem, "Exact modeling of non-gaussian measurement uncertainty in distribution system state estimation," *IEEE Trans. Instrum. Meas.*, vol. 72, pp. 1–11, 2023.

[9] D. Gerbec et al., "Allocation of the load profiles to consumers using probabilistic neural networks," *IEEE Trans. Power Syst.*, vol. 20, 2005.

[10] J. Zhang, J. Zhao, J. Yang, and J. Zhao, "Deep multi-fidelity bayesian data fusion for probabilistic distribution system voltage estimation with high penetration of pvs," *IEEE Trans. Power Syst.*, pp. 1–12, 2023.

[11] E. Razavi, A. A., S. D., L. G., N. G., and M. M., "Privacy-preserved framework for short-term probabilistic net energy forecasting," *IEEE Trans. on Industrial Informatics,* Oct 2022.

[12] R. Singh, B. Pal, and R. Jabr, "Distribution system state estimation through gaussian mixture model of the load as pseudo-measurement," *IET Gen., Transmiss. Distrib.*, vol. 4, no. 1, pp. 50–59, January 2010.

[13] J. J. Uhlmann, "The unscented Kalman filter for nonlinear estimation," *Proc. IEEE 2000 Adaptive Systems for Signal Processing, Communications, and Control Symposium, Canada*, 2000.

[14] S. J. Geetha, S. Chakrabarti, K. Rajawat and V. Terzija, "An Asynchronous Decentralized Forecasting-Aided State Estimator for Power Systems," *IEEE Trans. Power Syst.*, vol. 34, no. 4, Jul. 2019.

[15] R. Yu et al., "A Statistical Demand-Price Model With Its Application in Optimal Real-Time Price," *IEEE Trans. Smart Grid,* vol. 3,Dec. 2012.

[16] C. Muscas, F. Pilo, G. Pisano, and S. Sulis, "Optimal allocation of multichannel measurement devices for distribution state estimation," *IEEE Trans. Instrum. Meas.*, vol. 58, no. 6, pp. 1929–1937, Jun. 2009.

[17] PSL. (Dec. 2019). Micro PMU Data Sheet. [Online]. Available: https://www.powerstandards.com/download/micropmu-data-sheet/

[18] R. Dutta, S. J. Geetha, S. Chakrabarti and A. Sharma, "An L-1 Regularized Forecasting-Aided State Estimator for Active Distribution Networks," *IEEE Trans. on Smart Grid*, vol. 13, no. 1, Jan. 2022.

[19] M. M. Sheikh et al.,"Topology Guided Network Clustering and Allocation of Edge Estimation Points for Monitoring of Distribution Networks," *IEEE Trans. Smart Grid*, vol. 16, no. 5, Sept. 2025.

979-8-3315-8138-1